Relationship Between White Matter Hyperintensities, Cortical Thickness, and Cognition

Anil M. Tuladhar, MD; Andrew T. Reid, PhD; Elena Shumskaya, PhD; Karlijn F. de Laat, MD, PhD; Anouk G.W. van Norden, MD, PhD; Ewoud J. van Dijk, MD, PhD; David G. Norris, PhD; Frank-Erik de Leeuw, MD, PhD

Background and Purpose—White matter hyperintensities (WMH) are associated with clinically heterogeneous symptoms that cannot be explained by these lesions alone. It is hypothesized that these lesions are associated with distant cortical atrophy and cortical thickness network measures, which can result in an additional cognitive impairment. Here, we investigated the relationships between WMH, cortical thickness, and cognition in subjects with cerebral small vessel disease.

Methods—A total of 426 subjects with cerebral small vessel disease were included, aged between 50 and 85 years, without dementia, and underwent MRI scanning. Cortical thickness analysis was performed, and WMH were manually segmented. Graph theory was applied to examine the relationship between network measures and WMH, and structural covariance matrices were constructed using inter-regional cortical thickness correlations.

Results—Higher WMH load was related to lower cortical thickness in frontotemporal regions, whereas in paracentral regions, this was related to higher cortical thickness. Network analyses revealed that measures of network disruption were associated with WMH and cognitive performance. Furthermore, WMH in specific white matter tracts were related to regional-specific cortical thickness and network measures. Cognitive performances were related to cortical thickness in frontotemporal regions and network measures, and not to WMH, while controlling for cortical thickness.

Conclusions—These cross-sectional results suggest that cortical changes (regional-specific damage and network breakdown), mediated (in)directly by WMH (tract-specific damage) and other factors (eg, vascular risk factors), might lead to cognitive decline. These findings have implications in understanding the relationship between WMH, cortical morphology, and the possible attendant cognitive decline and eventually dementia. **(*Stroke*. 2015;46:425-432. DOI: 10.1161/STROKEAHA.114.007146.)**

Key Word: cognition

Cerebral small vessel disease includes, among others, white matter hyperintensities (WMH) of presumed vascular origin, which are commonly seen on cerebral MRI of healthy elderly individuals and are associated with vascular risk factors.[1,2] The underlying pathology of WMH is heterogeneous, ranging from mild demyelination to incomplete subcortical infarctions. These lesions are associated with cognitive and motor impairment,[3,4] although the exact mechanisms are not fully understood.

A possible mechanism by which WMH can result in clinical symptoms is by thinning of the previously connected cortex. This mechanism has recently been demonstrated in patients with cerebral autosomal–dominant arteriopathy with subcortical infarcts and leukoencephalopathy.[5,6] Also, a higher degree of cortical atrophy among individuals with higher burden of WMH has been demonstrated.[7–10] However, our understanding of this is limited because most previous studies used global measures[10] or showed conflicting results of the associations between WMH and regional brain atrophy. To date, several studies have conducted voxel-based morphometry showing that WMH are associated with regional cortical atrophy,[7,9,11] whereas other studies were conducted on patients with cerebral autosomal–dominant arteriopathy with subcortical infarcts and leukoencephalopathy.[5,6] An alternative method for examining the cortical morphology is the cortical thickness analysis.

Received August 20, 2014; final revision received December 1, 2014; accepted December 9, 2014.

From the Department of Neurology, Center for Neuroscience (A.M.T., A.G.W.v.N., E.J.v.D., F.-E.d.L.), Centre for Cognitive Neuroimaging (E.S., D.G.N.), Donders Institute for Brain, Cognition and Behaviour, Radboud University Nijmegen Medical Centre, Nijmegen, The Netherlands; Institute of Neuroscience and Medicine (INM-1), Research Center Julich, Julich, Germany (A.T.R.); Department of Neurology, HagaZiekenhuis Den Haag, Den Haag, The Netherlands (K.F.d.L.); Erwin L. Hahn Institute for Magnetic Resonance Imaging, University of Duisburg-Essen, Essen, Germany (D.G.N.); and MIRA Institute for Biomedical Technology and Technical Medicine, University of Twente, Enschede, The Netherlands (D.G.N.).

The online-only Data Supplement is available with this article at http://stroke.ahajournals.org/lookup/suppl/doi:10.1161/STROKEAHA.114.007146/-/DC1.

Correspondence to Frank-Erik de Leeuw, MD, PhD, Department of Neurology, Center for Neuroscience, Donders Institute for Brain, Cognition and Behaviour, Radboud University Nijmegen Medical Centre, Reinier Postlaan 4, PO Box 9101, 6500 HB, Nijmegen, The Netherlands. E-mail FrankErik.deLeeuw@radboudumc.nl

Another possible mechanism is that WMH might affect the cortex at the network level. The interactions between brain regions are important for efficient cognitive function. WMH could disrupt these interactions and might lead to network disruption at the cortical level and cognitive impairment. Graph theory can be used to examine the cortical morphology at the network level,[12] which can be constructed based on the interregional covariance of cortical thickness measures.[13,14] Graph theory typically captures the network organization, which provides information on the amount of integration and segregation among brain regions. It describes the brain regions as a set of nodes connected by edges based on the correlation analyses of cortical thickness measures. Alterations in network measures based on structural covariance have been found in various psychiatric and neurological disorders, including multiple sclerosis[15] and Alzheimer disease.[13]

Our objective is to investigate the relationships between WMH, cortical morphology (at the regional and network levels), and cognition in elderly, nondemented subjects with cerebral small vessel disease. We used cortical thickness analysis to identify cortical regions associated with WMH and performed graph theoretical analyses based on structural covariance to investigate the relationship between WMH, network measures, and cognition. We hypothesized that cortical thickness and network measures of structural covariance are related to the WMH and cognition and that the effects of WMH on cognitive performance would be mediated via cortical thickness.

Materials and Methods

Study Population

This study was embedded within the Radboud University

Nijmegen Diffusion tensor and MRI Cohort (RUN DMC) study, a prospective cohort study designed to investigate risk factors and cognitive, motor, and mood consequences of functional and structural brain changes as assessed by MRI among elderly with cerebral small vessel disease.[16] The inclusion criteria were (1) age between 50 and 85 years and (2) cerebral small vessel disease on neuroimaging. Small vessel disease was defined as the presence of WMH or lacune of presumed vascular origin. WMH were defined as white matter hyperintensity on fluid-attenuated inversion recovery images without prominent, or only faintly hypointensity on the T1-weighted images, except for gliosis, surrounding infarcts.[2] Lacunes were defined as hypointense areas >2 mm and ≤15 mm on fluid-attenuated inversion recovery and T1, ruling out enlarged perivascular spaces (≤2 mm, except around the anterior commissure, where perivascular spaces can be large) and infraputaminal pseudolacunes.[2] We did not intentionally include a cutoff value for WMH or lacunes to include participants across a wide range of disease severity. Exclusion criteria were (1) dementia, (2) Parkinson(ism), (3) intracranial hemorrhage, (4) life expectancy of <6 months, (5) intracranial space occupying lesion, (6) (psychiatric) disease interfering with cognitive testing or follow-up, (7) recent or current use of acetylcholinesterase inhibitors, neuroleptic agents, L-dopa, or dopa-a(nta)gonists, (8) WMH mimics (eg, multiple sclerosis and irradiation induced gliosis), (9) prominent visual or hearing impairment, (10) language barrier, and (11) MRI contraindications or known claustrophobia. Participants were selected for participation in the study by a 3-step approach. After reviewing the medical history, 1004 individuals were invited by letter. Of those 1004, 727 were eligible after contact by telephone and 525 agreed to participate. In 22 subjects, exclusion criteria were found during their visit to our research center (14 with unexpected claustrophobia, 1 died before MRI scanning, 1 was diagnosed with multiple sclerosis, in 1, there was a language barrier, 1 subject fulfilled the criteria for Parkinson disease, and 4 met the dementia criteria; Figure I in the online-only Data Supplement). For this study, 77 subjects were excluded because of failure of cortical thickness analysis pipeline (n=18), inadequate scan quality (n=4), and infarcts involving the cortex (n=55). More detailed information about the recruitment of the study sample can be found in the online-only Data Supplement and our study protocol.[16]

Cognitive Performances

All subjects underwent neuropsychological assessment covering many of the cognitive domains. These domains include mini-mental state examination, cognitive index, verbal and visuospatial memory, psychomotor speed, fluency, concept shifting, and attention. Further details are provided in the online-only Data Supplement.

Imaging Acquisition

Images were acquired using a 1.5 Tesla Siemens Magneton Sonata scanner (Siemens Medical Solutions, Erlangen, Germany), which included T1 3-dimensional magnetization-prepared rapid gradient-echo imaging (time repetition=2.25 s; time echo=3.68 ms; time interval=850 ms; flip angle=15°; voxelsize, 1.0×1.0×1.0 mm) and fluid-attenuated inversion recovery sequence (time repetition=9.00 s; time echo=84 ms; time interval=2.20 s; voxelsize, 1.0×1.2×5.0 mm, with a 1-mm interslice gap). All participants were scanned on the same scanner.

WMH Measurement

Two trained raters, blinded to clinical information, manually segmented the WMH. The inter-rater variability in a random sample of 10% revealed an intraclass correlation coefficient of 0.99. WMH volume was log-transformed because of skewed deviation. John Hopkinson University white matter atlas was used to calculate the WMH load in a set of white matter tracks (Table I in the online-only Data Supplement). To investigate the relationship between WMH and graph theoretical measures, we divided the study sample into quintiles based on WMH load. This resulted in 85 or 86 subjects per group. Clinical and imaging characteristics are given in Table and Table II in the online-only Data Supplement.

Cortical Thickness Analysis

For the cortical thickness analysis, the CIVET pipeline was used.[17] This pipeline consisted of registration of T1-images into stereotactic space, segmentation of images into background, gray matter, white matter, and cerebrospinal fluid mask, and identification of the inner and outer layers of the gray matter. Cortical thickness was measured as the distance between 2 corresponding vertices on the inner and outer surfaces. Finally, the individual images were registered to the surface template.

Structural Covariance Analysis

Structural covariance analysis is based on the covariance of the structural morphology, which can be either gray matter volume or cortical thickness. This approach is based on the assumption that the positive correlations are regarded as a connection between the regions.[12,14,18–20] Note that this approach does not infer direct anatomic connections between the regions.[21] The similarity of cortical morphology between the pairs of regions can still be a result of axonally connected brain regions.[22–26] A recent study reported that ≈40% of the cortical thickness correlations showed convergent diffusion connections at the group level, thus indicating that the cortical thickness correlations partly reflect underlying fiber connections.[23] Positive correlations can also arise as a result of parallel processing streams, rather than direct connectivity, such as mutually trophic, developmental, pathological, and maturational influences.[18,27–30] Thus, structural covariance can be regarded indicative, but not direct evidence, of an anatomic connection.

Surface segmentation in 78 regions was performed using the Automated Anatomical Labeling atlas (Table III in the online-only Data

Table. Baseline Characteristics

	Group 1, n=85	Group 2, n=85	Group 3, n=86	Group 4, n=85	Group 5, n=85
Clinical characteristics					
Age, y	59.9 (6.9)	61.3 (6.8)	64.3 (8.2)	68.4 (8.4)	71.5 (7.8)
Sex, female, %	44	46	45	52	45
Education (range)	5 (4–6)	5 (4–6)	5 (4–6)	5 (3–6)	5 (3–6)
Vascular risk factors					
Hypertension, %	56	62	69	79	92
Diabetes mellitus, %	12	9	16	16	14
Use of lipid-lowering drugs, %	45	44	38	45	47
Body mass index, kg/m^2	27.0 (4.7)	27.6 (4.0)	27.4 (4.3)	27.3 (4.3)	26.5 (3.7)
Smoking status					
Never, %	33	34	26	38	24
Former, %	53	48	59	48	60
Current, %	14	18	15	14	16
Neuroimaging characteristics					
Lacunes, number, %	7 (8%)	8 (9%)	12 (14%)	19 (22)	46 (54%)
WMH volume, mL	1.8 (0.6)	3.9 (0.7)	6.4 (1.0)	13.2 (3.4)	39.5 (22.6)
Cortical thickness, mm	3.21 (0.13)	3.19 (0.16)	3.19 (0.14)	3.10 (0.16)	3.04 (0.18)

Baseline characteristics per quintile of WMH load. Data represent means (SD), number (percentage), median (range), or percentages. Education score of 5 means 10–11 y of education. WMH indicates white matter hyperintensities.

Supplement).[31] For each region, mean cortical thickness was calculated and corrected for confounding factors (age, sex, interaction between age and sex, and overall mean cortical thickness) using multiple regression technique. The residuals were used to calculate the Pearson correlation coefficient, generating 78×78 matrix for each group. Positive inter-regional cortical thickness correlations correspond to synchronized cortical morphology, whereas negative correlations indicate the divergence of the cortical thickness between 2 cortical regions.

The absolute values of the inter-regional correlation matrices were thresholded into binarized matrices over the range of density thresholds (0.05–0.40, with 0.01 increment; Figure II in the online-only Data Supplement). If the correlation coefficient exceeded a certain threshold, it was considered a connection (or an edge) between 2 regions (or nodes) and assigned a value of 1. The threshold was related to the density. Density is defined as the total number of connections in a network divided by the possible number of connections. The density of a thresholded matrix thus refers to the proportion of its elements that have survived the thresholding, in other words, the proportion of nonzero elements. Similarly, for a graph, density refers to the number of edges in the graph as a proportion of all possible edges. The network measures are based on the group-wise networks.

We computed integrated mean path length, global efficiency, local efficiency, and clustering coefficient for each group to evaluate global network measures (Table IV in the online-only Data Supplement). Degree centrality, regional nodal efficiency, and betweenness centrality were calculated to investigate the network properties at the regional level.

Vascular Risk Factors

Following vascular risk factors were assessed: hypertension, diabetes mellitus, hypercholesterolemia, body mass index, and smoking status (online-only Data Supplement).

Statistical Analysis

Cortical thickness analyses were performed by SurfStat Toolbox (http://www.math.mcgill.ca/keith/surfstat) using a vertex-wise general linear model, controlling for age and sex. False discovery rate correction was applied at a q value of 0.05 to control for multiple comparisons.[32] The relationship between tract-specific WMH and cortical thickness was investigated while additionally controlling for the remaining WMH. Furthermore, we correlated the mean cortical thickness value of posterior cingulate cortex across participants with the whole brain using a vertex-wise general linear model, adjusted for age, sex, and overall mean cortical thickness (online-only Data Supplement and Figure III in the online-only Data Supplement). Inter-regional cortical thickness correlation analyses were performed after converting the correlations into z-scores using Fisher r-to-z transform. Only the pair-wise regions, significantly different from zero (P<0.01, false discovery rate–corrected), were considered for analyses. To test the network properties between groups based on WMH load, we applied a bootstrapping approach with 1000 replacements on cortical thickness values. For each bootstrap sample, we calculated network parameters and measured integrals (area under the curve) across the range of density. For group comparisons, we tested the resulting distribution statistically by performing an independent 2-sample t test (P<0.05, Bonferroni-corrected). Multiple regression analyses were performed to assess the relationship between cortical thickness, WMH, and cognition while controlling for age, sex, and educational level. Because mini-mental state examination was negatively skewed, we used Spearman ρ correlation coefficients while adjusting for age, sex, and education. Because the network parameters are highly correlated with each other, the integrated global efficiency was used as a marker of the network disruption. We investigated the relationship between integrated global efficiency, WMH, and cognition.

Supplemental Data

Supplemental material given in the online-only Data Supplement provides more information about study population, cognitive assessment, assessment of vascular risk factors, cortical thickness-analysis, construction of the structural covariance matrices, network properties and their formulae, and tract-specific WMH analyses.

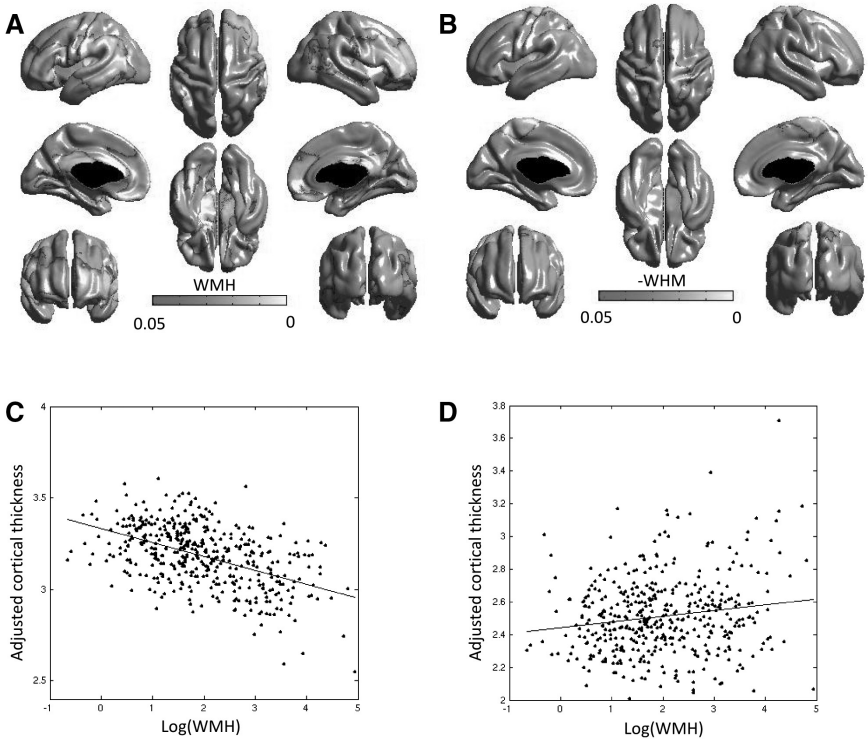

Figure 1. Relationship between white matter hyperintensities (WMH) and cortical thickness after removing the effects of age and sex. **A** and **B**, Negative and positive correlations between WMH and cortical thickness using a vertex-wise general linear model (P<0.05, false discovery rate–corrected), respectively. Relationship between WMH and mean cortical thickness of regions showing significant positive (**C**) and negative (**D**) correlations.

Results

Cortical Thickness Analyses

WMH load was negatively correlated with cortical thickness in bilateral frontotemporal regions, whereas WMH load was positively correlated with cortical thickness in the paracentral regions (P<0.05, false discovery rate–corrected; Figure 1). To investigate whether the relationship might be affected by outliers, we reanalyzed the data after removing the outliers (11 subjects), which were detected using the median absolute deviation method. The results remained similar, showing the positive correlations between cortical thickness and WMH in the same paracentral regions. Also, the results remained similar after additional adjustment for vascular risk factors.

Inter-Regional Cortical Thickness Correlation

Positive correlations between WMH load and inter-regional correlation coefficients were found between interhemispheric frontal and frontoparietal regions (P<0.01). Negative correlations were observed in various inter and intrahemispheric cortical regions, mainly encompassing long-range distance between the regions (Figure 2).

Cortical Thickness Network

Significant differences were found between each group comparison based on WMH load for global network properties (Figure 3; P<0.05, Bonferroni-corrected). Lower integrated global efficiency was related to a higher WMH quintile (r^2=0.997; P<0.001; d_f=3), whereas higher integrated path length, local efficiency, and clustering coefficient were related to a higher WMH quintile (r^2=0.984, P=0.001, d_f=3; r^2=0.981, P=0.003, d_f=3; and r^2=0.986, P=0.001, d_f=3, respectively). No significant associations between nodal efficiency, strength and betweenness centrality, and WMH were found (Figure IV in the online-only Data Supplement).

Tract-Specific WMH

Regional WMH load in corpus callosum (body and splenium and to lesser extent genu), internal capsule, corona radiata,

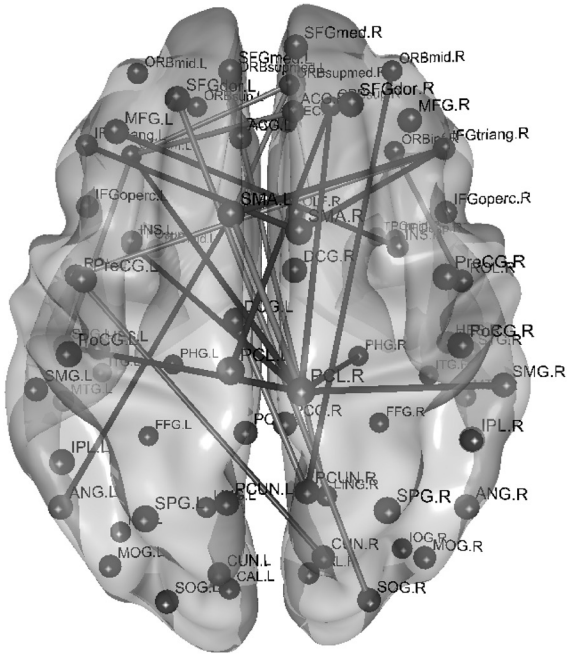

Figure 2. Graph visualization of the correlations between white matter hyperintensities (WMH) and inter-regional cortical thickness correlations. Red lines represent positive inter-regional cortical thickness correlations, and blue lines represent negative correlations in relation to WMH (P<0.01).

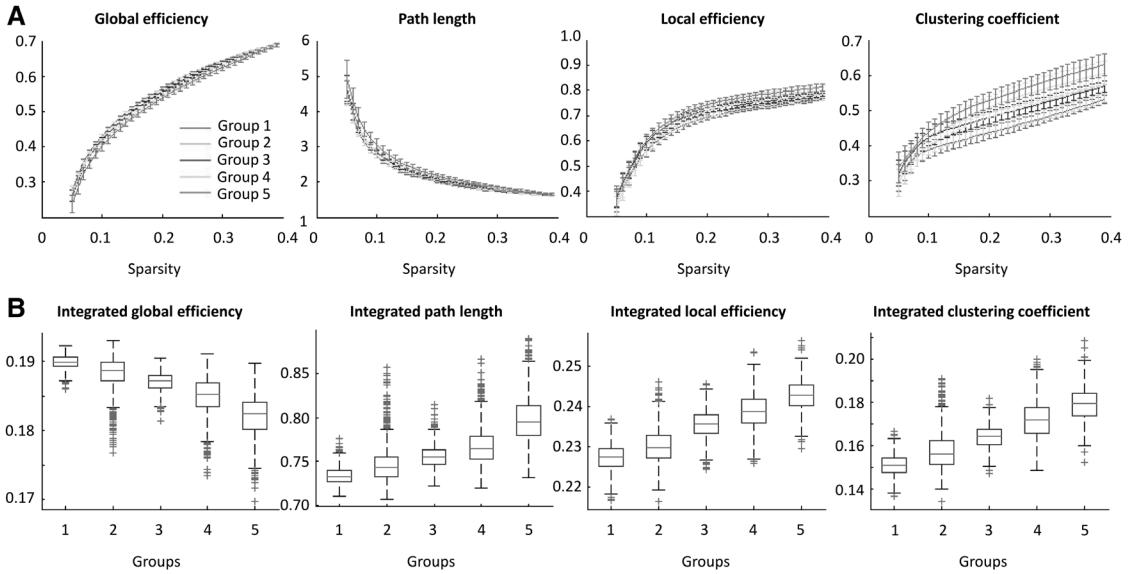

Figure 3. Network measures. **A**, Global efficiency, path length, local efficiency, and clustering coefficients as a function of density threshold (0.05 to 0.40) for each group. Differences between the groups can be seen across the range of density for each network measure. **B**, Integrated global efficiency, path length, local efficiency, and clustering coefficients for density threshold (0.05–0.40) using 1000 bootstrap samples for each group. Lower integrated global efficiency is observed in those with higher white matter hyperintensities (WMH), whereas higher integrated path length, local efficiency, and clustering coefficients are seen in those with higher WMH.

posterior thalamic radiation, superior longitudinal fasciculus, and external capsule was negatively correlated with cortical thickness in frontotemporal regions, whereas WMH load in corpus callosum, corona radiata, posterior thalamic radiation, sagittal stratum, and superior longitudinal fasciculus was positively correlated with cortical thickness in paracentral regions (P<0.05, false discovery rate–corrected and age- and sex-adjusted). Lower integrated global efficiency with higher WMH load was found in corpus callosum (body and splenium), corona radiata, and external capsule (P<0.05, Bonferroni-corrected).

Cognitive Functions

The cortical thickness of regions with significant negative association between WMH and cortical thickness was calculated. A thinner cortical thickness was related to poorer performance on various cognition domains while adjusted for age, sex, and education: cognitive index (β=0.23; P<0.001), mini-mental state examination (Spearman ρ=0.17; P<0.001), verbal memory (β=0.18; P<0.001), psychomotor speed (β=0.22; P<0.001), concept shifting (β=0.21; P<0.001), fluency (β=0.20; P<0.001), and attention (β=0.20; P<0.001). These relationships remained significant after additional adjustment for WMH. WMH was significantly related to these cognitive domains; however, after additionally controlling for cortical thickness, these relationships were not significant. To further establish mediation, we performed Sobel tests,[33] which revealed that cortical thickness mediated the association between WMH and above-mentioned cognitive performance (P<0.001). Cortical thickness or WMH was not related to visual memory. The integrated global efficiency was significantly related to all cognitive performances (P<0.05, uncorrected); however, after additional adjustment for WMH load, only the verbal memory (r^2=0.917; P=0.042; d_f=2) remained weakly significant. The role of the mediator was confirmed by Sobel test, which indicated that the association between WMH and verbal memory was mediated by global efficiency (z=−4.70; P<0.001).

Discussion

To the best of our knowledge, we investigated, for the first time, the relationship between WMH and cortical morphology using cortical thickness analyses and graph theoretical measures. We provided evidence for the relationship between WMH (global and tract-specific) and cortical thickness (regional and network levels) and for associations between WMH and cognition via the cortical thickness. These findings have implications for understanding the relationships between WMH, cortical morphology, and the possible attendant cognitive decline and dementia.

The strengths of this single-center study include its design, the homogeneous population that covers the whole spectrum of cerebral small vessel disease, its large sample size, the use of a single scanner, its structured and extensive cognitive assessment, and the manual segmentation of the WMH. However, several caveats and methodological considerations should be addressed. First, the pathological basis of cortical morphology is not well understood.[34] Several processes can occur simultaneously, but they need not necessarily be the same for each region or between the different groups. Second, although all analyses were performed in a linear fashion, cortical thickness changes in relation to WMH might not follow a linear trajectory. In agreement with other studies,[35] subjects with the highest WMH load showed significant lower scores on cognitive performance, suggesting a nonlinear relationship between WMH and cognition. Third, to investigate the role of WMH on the cortical thickness network, the mean cortical thickness value was regressed out

from the cortical thickness matrix. This is purposely done to remove any variance explained by global cortical thickness and to be consistent with other studies.[13,27] However, 1 caveat is that—possible spurious—correlations may be strengthened, which has been criticized for both cortical thickness and functional MRI studies. Additional analyses were conducted without regressing out the mean cortical thickness, which demonstrated the consistency of the results (Figure V in the online-only Data Supplement). Finally, these observations are based on cross-sectional data, which prevent us from making any causal inference or describing the temporal evolution of the events. This approach should be regarded as hypothesis generating because there were a large number of associations, hereby increasing the risk of false-positive results. Independent studies are therefore needed to confirm our findings. The RUN DMC study is a prospective study, and the follow-up is currently underway.

The clinical importance of WMH is indicated by their associations with cognitive impairment and increased risk of stroke recurrence, dementia, and death.[36] Furthermore, subjects with WMH and cognitive impairment are at higher risk for development of dementia when there is a concomitant presence of cortical atrophy.[37] Consistent with other studies,[38] we found that lower cortical thickness in frontotemporal regions was related to poorer cognitive performance independent of WMH. Involvement of cortical degeneration in frontal regions explains the frequently observed executive disturbances in subjects with small vessel disease.[39] Our study, in line with other studies,[6,9] suggests that the effects of WMH on cognitive performance might be mediated via a cortical thickness pathway.

In our study, higher WMH load was associated with lower cortical thickness in frontotemporal regions, indicating a regionally specific relationship. The pathophysiology of cortical atrophy in subjects with WMH is not completely understood. Subcortical lesions may conceivably result in disruptions of anatomic connections, leading to structural alterations of the cortex because of anterograde degeneration.[38] Damage to specific white matter tracks (among others corpus callosum, corona radiata, and superior longitudinal fasciculus), (in)directly connected to these regions,[40] may be responsible for this degeneration. Alternatively, cortical changes can produce axonal loss and demyelination because of Wallerian degeneration,[8] although some have criticized this reverse causation hypothesis.[41] Another explanation could be that the reduced cortical thickness in these nondemented participants might reflect early stages of the neurodegenerative process (eg, Alzheimer pathology) and that WMH is a coexisting pathology. Furthermore, reduced cortical thickness might also reflect microvascular damage within the cortex because of ischemia in the same arterial territory as WMH, although the magnitude of the associations between WMH and cortical thickness did not change markedly after adjustment for vascular risk factors. This suggests that other factors (eg, direct effects of WMH on cortical thickness or other risk factors) might be involved, independently of aging and vascular mechanisms.

In this study, higher WMH were also related to higher cortical thickness in paracentral regions. This could indicate compensatory mechanisms as a response to increasing WMH load, possibly reflecting an increased reliance on paracentral regions.[17] Increased cortical thickness has been found in several ageing studies[42,43] and in studies examining experience-[44] and training-related[45] changes, which may resemble the local plasticity. Another explanation could be the relative sparing, although this is usually characterized by the lack of association between cortical thickness and WMH. However, the functional implications of these associations still remain unclear. The interpretation of these results should be done carefully. It is also conceivable that changes of the signal properties in gray and white matter because of a high amount of myelinated projection fibers, microinfarcts, or progressive neuronal loss might influence cortical thickness measures,[42] which can lead to unexpected artifacts. Note that these findings are based on cross-sectional data. Future studies are warranted to investigate this relationship in more detail.

In our study, a higher WMH load was associated with lower global efficiency and longer path length. Global efficiency is mainly associated with long-distance connections. The long distance refers to multisynaptic pathways rather than geometrically remote because there are no actual distance weights. Higher global efficiency is considered as more effective inter-regional communication of information. If the cortical regions are affected through WMH, signal processing requires more synaptic relays, thereby resulting in decreased global efficiency. Our results showed that global efficiency was associated with cognitive performance. This suggests that network disruption might, at least in part, contribute to the occurrence of cognitive disturbances. The negative associations between WMH and cortical thickness in frontotemporal regions result in stronger inter-regional correlations, leading to a higher clustering coefficient and local efficiency with higher WMH load. This strengthens the notion that increased correlations and consequently, a higher local efficiency and clustering coefficient are because of coordinated thinning of the cortical morphology, rather than increased local connectivity. Nonetheless, WMH might be involved in the degeneration process of the cortical thickness-network, which might additionally contribute to the development of cognitive impairment.

In conclusion, this study of elderly nondemented subjects with cerebral small vessel disease shows a strong relationship between WMH, cortical thickness, and cognition. Cortical alterations (regional-specific damage and network breakdown), caused by direct or indirect effects of WMH (tract-specific damage) and other factors (eg, vascular risk factors), might lead to cognitive decline and eventually dementia. Future studies (preferably longitudinal) are needed for better understanding of the pathophysiology and the temporal evolution of WMH and cortical abnormalities and their effects on development of clinical symptoms.

Sources of Funding

Drs de Leeuw and van Dijk received personal fellowships from Dutch Brain Foundation (H04-12; F2009[1]-16) and clinical fellowships

from Netherlands Organization Scientific Research (40-00703-97-07197). Dr Leeuw received an Vidi innovational grant from the Netherlands Organization for Scientific Research (grant number 016.126.351). Dr Reid received research funding from National Institutes of Health and postdoctoral fellowship from Canadian Institutes of Health Research. This work was also supported by the Internationale Stichting Alzheimer Onderzoek.

Disclosures

None.

References

1. de Leeuw FE, de Groot JC, Oudkerk M, Witteman JC, Hofman A, van Gijn J, et al. A follow-up study of blood pressure and cerebral white matter lesions. *Ann Neurol*. 1999;46:827–833.
2. Wardlaw JM, Smith EE, Biessels GJ, Cordonnier C, Fazekas F, Frayne R, et al; STandards for ReportIng Vascular changes on nEuroimaging (STRIVE v1). Neuroimaging standards for research into small vessel disease and its contribution to ageing and neurodegeneration. *Lancet Neurol*. 2013;12:822–838. doi: 10.1016/S1474-4422(13)70124-8.
3. de Laat KF, Tuladhar AM, van Norden AG, Norris DG, Zwiers MP, de Leeuw FE. Loss of white matter integrity is associated with gait disorders in cerebral small vessel disease. *Brain*. 2011;134(pt 1):73–83. doi: 10.1093/brain/awq343.
4. Prins ND, van Dijk EJ, den Heijer T, Vermeer SE, Jolles J, Koudstaal PJ, et al. Cerebral small-vessel disease and decline in information processing speed, executive function and memory. *Brain*. 2005;128(pt 9):2034–2041. doi: 10.1093/brain/awh553.
5. Duering M, Righart R, Csanadi E, Jouvent E, Hervé D, Chabriat H, et al. Incident subcortical infarcts induce focal thinning in connected cortical regions. *Neurology*. 2012;79:2025–2028. doi: 10.1212/WNL.0b013e3182749f39.
6. Righart R, Duering M, Gonik M, Jouvent E, Reyes S, Hervé D, et al. Impact of regional cortical and subcortical changes on processing speed in cerebral small vessel disease. *Neuroimage Clin*. 2013;2:854–861. doi: 10.1016/j.nicl.2013.06.006.
7. Rossi R, Boccardi M, Sabattoli F, Galluzzi S, Alaimo G, Testa C, et al. Topographic correspondence between white matter hyperintensities and brain atrophy. *J Neurol*. 2006;253:919–927. doi: 10.1007/s00415-006-0133-z.
8. Godin O, Maillard P, Crivello F, Alpérovitch A, Mazoyer B, Tzourio C, et al. Association of white-matter lesions with brain atrophy markers: the three-city Dijon MRI study. *Cerebrovasc Dis*. 2009;28:177–184. doi: 10.1159/000226117.
9. Raji CA, Lopez OL, Kuller LH, Carmichael OT, Longstreth WT Jr, Gach HM, et al. White matter lesions and brain gray matter volume in cognitively normal elders. *Neurobiol Aging*. 2012;33:834.e7–834.e16.
10. Appelman AP, Exalto LG, van der Graaf Y, Biessels GJ, Mali WP, Geerlings MI. White matter lesions and brain atrophy: more than shared risk factors? A systematic review. *Cerebrovasc Dis*. 2009;28:227–242. doi: 10.1159/000226774.
11. Wen W, Sachdev PS, Chen X, Anstey K. Gray matter reduction is correlated with white matter hyperintensity volume: a voxel-based morphometric study in a large epidemiological sample. *Neuroimage*. 2006;29:1031–1039. doi: 10.1016/j.neuroimage.2005.08.057.
12. Bullmore E, Sporns O. Complex brain networks: graph theoretical analysis of structural and functional systems. *Nat Rev Neurosci*. 2009;10:186–198. doi: 10.1038/nrn2575.
13. He Y, Chen Z, Evans A. Structural insights into aberrant topological patterns of large-scale cortical networks in Alzheimer's disease. *J Neurosci*. 2008;28:4756–4766. doi: 10.1523/JNEUROSCI.0141-08.2008.
14. Worsley KJ, Chen JI, Lerch J, Evans AC. Comparing functional connectivity via thresholding correlations and singular value decomposition. *Philos Trans R Soc Lond B Biol Sci*. 2005;360:913–920. doi: 10.1098/rstb.2005.1637.
15. He Y, Dagher A, Chen Z, Charil A, Zijdenbos A, Worsley K, et al. Impaired small-world efficiency in structural cortical networks in multiple sclerosis associated with white matter lesion load. *Brain*. 2009;132(pt 12):3366–3379. doi: 10.1093/brain/awp089.
16. van Norden AG, de Laat KF, Gons RA, van Uden IW, van Dijk EJ, van Oudheusden LJ, et al. Causes and consequences of cerebral small vessel disease. The RUN DMC study: a prospective cohort study. Study rationale and protocol. *BMC Neurol*. 2011;11:29. doi: 10.1186/1471-2377-11-29.
17. Reid AT, van Norden AG, de Laat KF, van Oudheusden LJ, Zwiers MP, Evans AC, et al. Patterns of cortical degeneration in an elderly cohort with cerebral small vessel disease. *Hum Brain Mapp*. 2010;31:1983–1992. doi: 10.1002/hbm.20994.
18. Lerch JP, Worsley K, Shaw WP, Greenstein DK, Lenroot RK, Giedd J, et al. Mapping anatomical correlations across cerebral cortex (MACACC) using cortical thickness from MRI. *Neuroimage*. 2006;31:993–1003. doi: 10.1016/j.neuroimage.2006.01.042.
19. Evans AC. Networks of anatomical covariance. *Neuroimage*. 2013;80:489–504. doi: 10.1016/j.neuroimage.2013.05.054.
20. Alexander-Bloch A, Giedd JN, Bullmore E. Imaging structural co-variance between human brain regions. *Nat Rev Neurosci*. 2013;14:322–336. doi: 10.1038/nrn3465.
21. Bernhardt BC, Hong S, Bernasconi A, Bernasconi N. Imaging structural and functional brain networks in temporal lobe epilepsy. *Front Hum Neurosci*. 2013;7:624. doi: 10.3389/fnhum.2013.00624.
22. Tijms BM, Möller C, Vrenken H, Wink AM, de Haan W, van der Flier WM, et al. Single-subject grey matter graphs in Alzheimer's disease. *PLoS One*. 2013;8:e58921. doi: 10.1371/journal.pone.0058921.
23. Gong G, He Y, Chen ZJ, Evans AC. Convergence and divergence of thickness correlations with diffusion connections across the human cerebral cortex. *Neuroimage*. 2012;59:1239–1248. doi: 10.1016/j.neuroimage.2011.08.017.
24. Hilgetag CC, Kaiser M. Clustered organization of cortical connectivity. *Neuroinformatics*. 2004;2:353–360. doi: 10.1385/NI:2:3:353.
25. Van Essen DC. A tension-based theory of morphogenesis and compact wiring in the central nervous system. *Nature*. 1997;385:313–318. doi: 10.1038/385313a0.
26. Mechelli A, Friston KJ, Frackowiak RS, Price CJ. Structural covariance in the human cortex. *J Neurosci*. 2005;25:8303–8310. doi: 10.1523/JNEUROSCI.0357-05.2005.
27. Bernhardt BC, Chen Z, He Y, Evans AC, Bernasconi N. Graph-theoretical analysis reveals disrupted small-world organization of cortical thickness correlation networks in temporal lobe epilepsy. *Cereb Cortex*. 2011;21:2147–2157. doi: 10.1093/cercor/bhq291.
28. Khundrakpam BS, Reid A, Brauer J, Carbonell F, Lewis J, Ameis S, et al; Brain Development Cooperative Group. Developmental changes in organization of structural brain networks. *Cereb Cortex*. 2013;23:2072–2085. doi: 10.1093/cercor/bhs187.
29. Zhang K, Sejnowski TJ. A universal scaling law between gray matter and white matter of cerebral cortex. *Proc Natl Acad Sci U S A*. 2000;97:5621–5626. doi: 10.1073/pnas.090504197.
30. Wright IC, Sharma T, Ellison ZR, McGuire PK, Friston KJ, Brammer MJ, et al. Supra-regional brain systems and the neuropathology of schizophrenia. *Cereb Cortex*. 1999;9:366–378.
31. Tzourio-Mazoyer N, Landeau B, Papathanassiou D, Crivello F, Etard O, Delcroix N, et al. Automated anatomical labeling of activations in SPM using a macroscopic anatomical parcellation of the MNI MRI single-subject brain. *Neuroimage*. 2002;15:273–289. doi: 10.1006/nimg.2001.0978.
32. Genovese CR, Lazar NA, Nichols T. Thresholding of statistical maps in functional neuroimaging using the false discovery rate. *Neuroimage*. 2002;15:870–878. doi: 10.1006/nimg.2001.1037.
33. Preacher KJ, Hayes AF. SPSS and SAS procedures for estimating indirect effects in simple mediation models. *Behav Res Methods Instrum Comput*. 2004;36:717–731.
34. Zatorre RJ, Fields RD, Johansen-Berg H. Plasticity in gray and white: neuroimaging changes in brain structure during learning. *Nat Neurosci*. 2012;15:528–536. doi: 10.1038/nn.3045.
35. de Groot JC, de Leeuw FE, Oudkerk M, van Gijn J, Hofman A, Jolles J, et al. Cerebral white matter lesions and cognitive function: the Rotterdam Scan Study. *Ann Neurol*. 2000;47:145–151.
36. Debette S, Markus HS. The clinical importance of white matter hyperintensities on brain magnetic resonance imaging: systematic review and meta-analysis. *BMJ*. 2010;341:c3666.
37. Smith EE, Egorova S, Blacker D, Killiany RJ, Muzikansky A, Dickerson BC, et al. Magnetic resonance imaging white matter hyperintensities and brain volume in the prediction of mild cognitive impairment and dementia. *Arch Neurol*. 2008;65:94–100. doi: 10.1001/archneurol.2007.23.
38. Du AT, Schuff N, Chao LL, Kornak J, Ezekiel F, Jagust WJ, et al. White matter lesions are associated with cortical atrophy more than entorhinal and hippocampal atrophy. *Neurobiol Aging*. 2005;26:553–559. doi: 10.1016/j.neurobiolaging.2004.05.002.

39. Gunning-Dixon FM, Raz N. The cognitive correlates of white matter abnormalities in normal aging: a quantitative review. *Neuropsychology*. 2000;14:224–232.
40. Glickstein M, Berlucchi G. Classical disconnection studies of the corpus callosum. *Cortex*. 2008;44:914–927.
41. Schmidt R, Ropele S, Enzinger C, Petrovic K, Smith S, Schmidt H, et al. White matter lesion progression, brain atrophy, and cognitive decline: the Austrian stroke prevention study. *Ann Neurol*. 2005;58:610–616. doi: 10.1002/ana.20630.
42. Fjell AM, Westlye LT, Amlien I, Espeseth T, Reinvang I, Raz N, et al. High consistency of regional cortical thinning in aging across multiple samples. *Cereb Cortex*. 2009;19:2001–2012. doi: 10.1093/cercor/bhn232.
43. Ziegler DA, Piguet O, Salat DH, Prince K, Connally E, Corkin S. Cognition in healthy aging is related to regional white matter integrity, but not cortical thickness. *Neurobiol Aging*. 2010;31:1912–1926. doi: 10.1016/j.neurobiolaging.2008.10.015.
44. Maguire EA, Gadian DG, Johnsrude IS, Good CD, Ashburner J, Frackowiak RS, et al. Navigation-related structural change in the hippocampi of taxi drivers. *Proc Natl Acad Sci U S A*. 2000;97:4398–4403. doi: 10.1073/pnas.070039597.
45. Scholz J, Klein MC, Behrens TE, Johansen-Berg H. Training induces changes in white-matter architecture. *Nat Neurosci*. 2009;12:1370–1371. doi: 10.1038/nn.2412.

Relationship Between White Matter Hyperintensities, Cortical Thickness, and Cognition

Anil M. Tuladhar, Andrew T. Reid, Elena Shumskaya, Karlijn F. de Laat, Anouk G.W. van Norden, Ewoud J. van Dijk, David G. Norris and Frank-Erik de Leeuw

Stroke. 2015;46:425-432; originally published online January 8, 2015;
doi: 10.1161/STROKEAHA.114.007146
Stroke is published by the American Heart Association, 7272 Greenville Avenue, Dallas, TX 75231

Print ISSN: 0039-2499. Online ISSN: 1524-4628

SUPPLEMENTARY MATERIAL

Study population

This study is embedded within the "Radboud University Nijmegen Diffusion tensor and MRI Cohort" (RUN DMC) study, a prospective cohort study that was designed to investigate risk factors and cognitive, motor and mood consequences of functional and structural brain changes as assessed by MRI among elderly with cerebral small vessel disease.[1] Symptoms of small vessel disease can be acute, such as TIAs or lacunar infarcts, or subacute manifestations such as cognitive, gait and/or mood disturbances. Because the onset of small vessel disease is often insidious, clinically heterogeneous, it has been suggested that the selection of subjects with small vessel disease should be based on these more consistent brain imaging features. Small vessel disease was defined as the presence of WMH and/or lacunes. WMH were defined as white matter hyperintensity on FLAIR-images without prominent, or only faintly hypo-intensity on the T1-weighted images, except for gliosis surrounding infarcts.[2] Lacunes of presumed vascular origin were defined as hypo-intense areas > 2 mm and ≤ 15mm on FLAIR and T1, ruling out enlarged perivascular spaces (≤ 2 mm, except around the anterior commissure, where perivascular spaces can be large) and infraputaminal pseudolacunes.[2, 3]

Consecutive patients referred to the Department of Neurology between October 2002 and November 2006 were selected for participation. The above-mentioned acute or subacute clinical symptoms of small vessel disease were assessed by standardized structured assessments. Patients who were eligible because of a lacunar syndrome were included only >6 months after the event to avoid acute effects on the outcome.

The inclusion criteria were 1) age between 50 and 85 years and 2) cerebral small vessel disease on neuroimaging (white matter hyperintensities and/or lacunar infarct(s)). Exclusion criteria were (1) dementia; (2) Parkinson(ism); (3) intracranial haemorrhage; (4) life expectancy of < 6 months; (5) intracranial space occupying lesion; (6) (psychiatric) disease interfering with cognitive testing or follow-up; (7) recent or current use of acetylcholine-esterase inhibitors, neuroleptic agents, L-dopa or dopa-a(nta)gonists,; (8) WMH mimics (e.g. multiple sclerosis and irradiation induced gliosis); (9) prominent visual or hearing impairment; (10) language barrier; (11) MRI contraindications or known claustrophobia.

Participants were selected for participation in the study by a three-step approach. After reviewing the medical history, 1004 individuals were invited by letter. Of those 1004, 727 were eligible after contact by telephone phone and 525 agreed to participate. In 22 subjects exclusion criteria were found during their visit to our research centre (14 with unexpected claustrophobia, 1 died before MRI scanning, 1 was diagnosed with multiple sclerosis, in 1 there was a language barrier, 1 subject fulfilled the criteria for Parkinson's disease and 4 met the dementia criteria), yielding a response of 71.3% (503/705) for the original cohort of the study. See Supplemental figure I for flowchart of the study design. These 503 individuals had symptoms of TIA or lacunar syndrome (n=219), cognitive disturbances (n=245), motor disturbances (n=97), depressive symptoms (n=100) or a combination thereof. All participants signed an informed consent form. More detailed information about the recruitment of the study sample can be found in our study protocol.[1]

Cognitive performances

All subjects underwent neuropsychological assessment covering many of the cognitive domains. Raw test scores were transformed to z-scores and were used to calculate performance in seven cognitive domains: (1) Global cognitive function: evaluated by Mini Mental State Examination and cognitive index. Cognitive index is a compound score, including the mean of the z-scores of the 1-letter subtask of the Paper-Pencil Memory Scanning Task, the mean of the reading subtask of the Stroop test, the mean of the Symbol-Digit Substitution Task and the mean of the added score on the three learning trials and the delayed recall of the Rey Auditory Verbal Learning Test (RAVLT).[4] (2) Verbal memory: mean of the added score on the three learning trials and the delayed recall of the RAVLT. (3) Visuospatial memory: compound score of the mean of the immediate recall trial and the delayed recall trial of the Rey's Complex Figure Test. (4) Psychomotor speed: mean of the z-scores of the 1-letter subtask of the Paper-Pencil Memory Scanning Task, the reading subtask of the Stroop test and the Symbol-Digit Substitution Task. (5) Fluency: mean of both verbal fluency tasks. (6) Concept shifting: z-score of the third subtask of the Stroop, the inference task. (7) Attention: compound score of the total time of the Verbal Series Attention Test. Baseline cognitive characteristics are given in Supplemental Table II.

Vascular risk factors

Hypertension was defined as systolic blood pressure ≥ 140 mmHg or diastolic blood pressure ≥ 90 mmHg and/or use of antihypertensive drugs. Blood pressures were measured 3 times in supine position after 5 minutes rest. The average of these 3 measures was used. Diabetes and hypercholesterolemia were considered to be present if the participant was taking anti-diabetic or lipid-lowering drugs for high cholesterol. Body mass index (BMI) was calculated as weight divided by height (in meters) squared. The smoking status was obtained through standardized questionnaires, which was checked during the interview.

Cortical thickness analysis

In this study, we employed cortical thickness analysis. Cortical thickness analysis might provide a more sensitive measure in detecting alterations in cortical morphology than volumetric approach[5] and has been proven to be reliable in terms of spatial localization and magnitude of cortical thickness measurements.[6] For the cortical thickness analysis, the CIVET pipeline was employed.[7] First, the structural T1 images were registered into stereotactic space using a nine-parameter linear transformation,[8] corrected for the non-uniformity artifacts using the N3 algorithm.[9] Second, the images were segmented into background, grey matter, white matter and cerebrospinal fluid mask.[10] Third, the inner and outer layers of the grey matter were determined using the Constrained Laplacian-based Automated Segmentation with Proximities (CLASP) procedure.[11, 12] The CIVET pipeline resulted in a triangulated cortex, which contains 40.960 vertices per hemisphere. The cortical thickness was measured as the distance between the two corresponding vertices on the inner and outer surfaces. Finally, the individual images were registered to the surface template, obtained using an iterative group template registration algorithm to allow intersubject comparisons.[13]

Construction of the structural covariance matrices

The cortical surface segmentation was performed using the Automated Anatomical Labeling (AAL) atlas,[14] resulting in 78 cortical regions (Supplemental Table III). Since the cortical thickness analysis is based upon cortical surface model, we included only those 78 AAL regions defined for the neocortex. For each AAL region, we calculated the mean cortical thickness, after which various confounding factors (age, gender, interaction between age and gender, and overall mean cortical thickness) were removed from the cortical thickness data using a multiple regression technique. The residuals were then used to calculate the Pearson's correlation coefficient for every pair-wise region, hereby generating 78 by 78 interregional correlation matrix for each group.

The density is defined as the number of edges (K) in the network (or a graph G) divided by the possible number of edges $N(N\text{-}1)/2$. We binarized the matrices at a fixed density in order to obtain the same size of the graph for each group, which is necessary to statistically compare topological graph measures between groups.[15] The correlation matrices were then thresholded into binarized matrices over the range of density values 0.05 - 0.40, with 0.01 increments, which typically show small-world organization while minimizing the presence of spurious edges in the graph.[15, 16] If the correlation coefficient exceeded a certain threshold, it was considered a "connection" (or an edge) between two regions (or nodes) and assigned a value of 1. Comparisons between graph measures require that the densities of the graphs be the same; otherwise trivial differences are expected which have no relation to the graph's topology.[17] However, there is no clear rationale for choosing which density at which to threshold. To address this issue, we performed our analyses over a range of densities (0.05-0.40, with 0.01 increment). Supplemental Figure II displays the automated anatomical labeling (AAL) template, interregional cortical thickness correlation and binarized matrices after thresholding at a fixed density. In all five groups, the correlation matrices show similar structural covariance patterns on visual inspection.

Several studies have demonstrated that the default mode network can be reproduced using the structural covariance analysis.[18-20] To reproduce these findings with our cortical thickness data, we extracted the mean cortical thickness values of the posterior cingulate cortex (PCC), which is considered as the core hub of the default mode network. We then correlated this cortical thickness value across participants with the whole brain using vertex-wise general linear model, adjusted for age, gender and overall mean cortical thickness. A significant structural covariance pattern with the PCC seed ($p < 0.05$, corrected for multiple comparisons) was found, at least in part consistent with the default mode network (Supplemental Figure III).

Network analysis

We computed the mean path length, global efficiency, local efficiency and clustering coefficient for each group at a fixed density using in-house Matlab scripts. Next, we computed the integration of these network parameters across the density to evaluate the global network characteristics.[15] The formulae for these parameters are displayed in Supplemental Table IV. Mean path length is the average number of steps along the shortest

paths for all possible pairs of a network (or a graph). The global efficiency of the network is defined as the sum of inverse of the shortest path length between two nodes.[21] Path length and global efficiency represent the global connectivity, indicating the efficiency of long-distance communication of information between the nodes. The local efficiency for each node is the global efficiency of the neighborhood subgraph of a node.[21] The local efficiency is related to the clustering coefficient, which measures the degree to which a node's neighbors tend to connect to each other. The local efficiency and clustering coefficients for the graph are calculated by node-wise averaging of these parameters. These measures represent the local connectivity of the network.

To investigate the network properties on the regional level, we calculated the degree centrality (number of edges adjacent to a node), regional nodal efficiency and betweenness centrality. The nodal efficiency is defined as the average inverse of shortest path length between a node and other nodes in the graph.[15] The betweenness centrality of a node is calculated as the number of all shortest paths in the graph that pass through the node.[22] This measures the participation of the node in the graph with respect to information transfer and can identify critical nodes in the graph. Supplemental Figure IV displays only the cortical regions if the score for the respective parameters is higher than the mean plus one standard deviation, thus showing the highest ranked brain regions for each group (the highest nodal strength, nodal efficiency and betweenness centrality).

To investigate the role of WMH on the cortical thickness network, the mean cortical thickness value was regressed out from the cortical thickness matrix. This is purposely done to remove any variance explained by global cortical thickness and to be consistent with other studies. However, one caveat is that– possible spurious – correlations may be strengthened.[23] To test this possibility, we performed additional analyses, in which cortical thickness-matrix was constructed without regressing out the mean cortical thickness. These additional results demonstrated the consistency of the results (Supplemental Figure V).

Tract-specific WMH

The JHU white matter atlas was used to calculate the WMH in the white matter tract. For this, we registered the atlas to the native T1 image using the inverse of the transformation matrix obtained from the non-linear registration of the skulled-stripped T1 images to MNI space. The WMH map was registered to the native T1 image, which then used to calculate the WMH load in a specific white matter tract. The highest WMH load in group 5 was found in the corona radiata (WMH = 6.04 ml), followed by posterior thalamic radiation (WMH = 2.88 ml), corpus callosum splenium (WMH = 1.33 ml), body (WMH = 0.98 ml) and genu (WMH = 0.96 ml) and internal capsule (WMH = 1.16 ml). Supplemental Table I shows the volume of WMH per fiber tract for each group based on the WMH load.

References

1. van Norden AG, de Laat KF, Gons RA, van Uden IW, van Dijk EJ, van Oudheusden LJ, et al. Causes and consequences of cerebral small vessel disease. The run dmc study: A prospective cohort study. Study rationale and protocol. *BMC neurology*. 2011;11:29
2. Wardlaw JM, Smith EE, Biessels GJ, Cordonnier C, Fazekas F, Frayne R, et al. Neuroimaging standards for research into small vessel disease and its contribution to ageing and neurodegeneration. *The Lancet. Neurology*. 2013;12:822-838
3. Herve D, Mangin J-F, Molko N, Bousser M-G, Chabriat H. Shape and volume of lacunar infarcts: A 3d mri study in cerebral autosomal dominant arteriopathy with subcortical infarcts and leukoencephalopathy. *Stroke*. 2005;36:2384-2388
4. de Groot JC, de Leeuw FE, Oudkerk M, van Gijn J, Hofman A, Jolles J, et al. Cerebral white matter lesions and cognitive function: The rotterdam scan study. *Annals of neurology*. 2000;47:145-151
5. Hutton C, Draganski B, Ashburner J, Weiskopf N. A comparison between voxel-based cortical thickness and voxel-based morphometry in normal aging. *NeuroImage*. 2009;48:371-380
6. Dickerson BC, Fenstermacher E, Salat DH, Wolk DA, Maguire RP, Desikan R, et al. Detection of cortical thickness correlates of cognitive performance: Reliability across mri scan sessions, scanners, and field strengths. *NeuroImage*. 2008;39:10-18
7. Reid AT, van Norden AG, de Laat KF, van Oudheusden LJ, Zwiers MP, Evans AC, et al. Patterns of cortical degeneration in an elderly cohort with cerebral small vessel disease. *Human brain mapping*. 2010;31:1983-1992
8. Collins DL, Neelin P, Peters TM, Evans AC. Automatic 3d intersubject registration of mr volumetric data in standardized talairach space. *Journal of computer assisted tomography*. 1994;18:192-205
9. Sled JG, Zijdenbos AP, Evans AC. A nonparametric method for automatic correction of intensity nonuniformity in mri data. *IEEE transactions on medical imaging*. 1998;17:87-97
10. Zijdenbos AP, Forghani R, Evans AC. Automatic "pipeline" analysis of 3-d mri data for clinical trials: Application to multiple sclerosis. *IEEE transactions on medical imaging*. 2002;21:1280-1291
11. Kim JS, Singh V, Lee JK, Lerch J, Ad-Dab'bagh Y, MacDonald D, et al. Automated 3-d extraction and evaluation of the inner and outer cortical surfaces using a laplacian map and partial volume effect classification. *NeuroImage*. 2005;27:210-221
12. MacDonald D, Kabani N, Avis D, Evans AC. Automated 3-d extraction of inner and outer surfaces of cerebral cortex from mri. *NeuroImage*. 2000;12:340-356
13. Lyttelton O, Boucher M, Robbins S, Evans A. An unbiased iterative group registration template for cortical surface analysis. *NeuroImage*. 2007;34:1535-1544
14. Tzourio-Mazoyer N, Landeau B, Papathanassiou D, Crivello F, Etard O, Delcroix N, et al. Automated anatomical labeling of activations in spm using a macroscopic anatomical parcellation of the mni mri single-subject brain. *NeuroImage*. 2002;15:273-289
15. Achard S, Bullmore E. Efficiency and cost of economical brain functional networks. *PLoS computational biology*. 2007;3:e17
16. Bassett DS, Bullmore E, Verchinski BA, Mattay VS, Weinberger DR, Meyer-Lindenberg A. Hierarchical organization of human cortical networks in health and schizophrenia. *The Journal of neuroscience : the official journal of the Society for Neuroscience*. 2008;28:9239-9248
17. van Wijk BC, Stam CJ, Daffertshofer A. Comparing brain networks of different size and connectivity density using graph theory. *PloS one*. 2010;5:e13701
18. Seeley WW, Crawford RK, Zhou J, Miller BL, Greicius MD. Neurodegenerative diseases target large-scale human brain networks. *Neuron*. 2009;62:42-52

19. Zielinski BA, Gennatas ED, Zhou J, Seeley WW. Network-level structural covariance in the developing brain. *Proceedings of the National Academy of Sciences of the United States of America*. 2010;107:18191-18196
20. Spreng RN, Turner GR. Structural covariance of the default network in healthy and pathological aging. *The Journal of neuroscience : the official journal of the Society for Neuroscience*. 2013;33:15226-15234
21. Latora V, Marchiori M. Efficient behavior of small-world networks. *Physical review letters*. 2001;87:198701
22. Freeman LC. Set of measures of centrality based on betweenness. *Sociometry*. 1977;40:35-41
23. Murphy K, Birn RM, Handwerker DA, Jones TB, Bandettini PA. The impact of global signal regression on resting state correlations: Are anti-correlated networks introduced? *NeuroImage*. 2009;44:893-905

Supplemental Table I: Volume of white matter hyperintensities per fiber tract.

	Group 1 N = 85	Group 2 N = 85	Group 3 N = 86	Group 4 N = 85	Group 5 N = 85
Corpus callosum – Genu (ml)	0.12 (0.06)	0.22 (0.11)	0.31(0.12)	0.50 (0.25)	0.96 (0.55)
Corpus callosum – Body (ml)	0.01 (0.03)	0.05 (0.07)	0.08 (0.11)	0.20 (0.18)	0.98 (1.22)
Corpus callosum - Splenium (ml)	0.02 (0.03)	0.05 (0.06)	0.10 (0.15)	0.25 (0.25)	1.33 (1.27)
Corticospinal tract (ml)	0.01 (0.02)	0.01 (0.02)	0.03 (0.04)	0.06 (0.21)	0.07 (0.12)
Internal capsule (ml)	0.02 (0.03)	0.06 (0.10)	0.11 (0.16)	0.25 (0.26)	1.16 (1.13)
Corona radiata (ml)	0.15 (0.10)	0.31 (0.16)	0.56 (0.26)	1.37 (0.72)	6.04 (4.90)
Posterior thalamic radiation (ml)	0.05 (0.06)	0.15 (0.16)	0.31 (0.26)	0.71 (0.48)	2.88 (1.90)
Sagittal stratum (ml)	0.00 (0.00)	0.01 (0.08)	0.01 (0.02)	0.03 (0.06)	0.22 (0.39)
External capsule (ml)	0.01 (0.01)	0.01 (0.03)	0.03 (0.04)	0.09 (0.12)	0.39 (0.46)
Superior longitudinal fasciculus (ml)	0.01 (0.01)	0.02 (0.03)	0.04 (0.04)	0.08 (0.06)	0.35 (0.27)
Tapetum (ml)	0.02 (0.04)	0.07 (0.08)	0.15 (0.16)	0.33 (0.28)	1.00 (0.46)

Data represent means (standard deviation).

Supplemental Table II. Baseline cognitive characteristics

	Group 1 N = 85	Group 2 N = 85	Group 3 N = 86	Group 4 N = 85	Group 5 N = 85	Overall N = 426
Cognitive performance						
Global cognitive performance						
MMSE (raw scores)	29 (28-30)	29 (28-30)	29 (27-29)	28 (26-29)	27 (26-29)	29 (27-30)
MMSE (z-scores)	0.21 (0.98)	0.33 (0.83)	0.01 (0.95)	-0.10 (1.05)	-0.45 (1.02)	
Cognitive index (z-scores)	0.28 (0.60)	0.17 (0.68)	0.02 (0.79)	-0.13 (0.70)	-0.42 (0.73)	
Verbal memory (z-scores)	0.15 (0.88)	0.20 (0.86)	0.08 (0.88)	-0.06 (0.90)	-0.41 (0.84)	
Visual memory (z-scores)	0.17 (0.91)	0.14 (0.94)	0.05 (1.09)	-0.16 (0.90)	-0.22 (1.03)	
Fluency (z-scores)	0.23 (0.77)	0.21 (1.03)	-0.04 (0.94)	-0.07 (0.92)	-0.35 (0.81)	
Attention (z-scores)	0.18 (0.94)	0.20 (0.83)	-0.08 (0.88)	-0.06 (1.04)	-0.42 (1.17)	
Concept shifting (z-scores)	0.32 (0.81)	0.28 (0.77)	0.10 (0.88)	-0.23 (1.17)	-0.53 (1.08)	
Psychomotor speed (z-scores)	0.37 (0.63)	0.17 (0.75)	0.00 (0.94)	-0.15 (0.76)	-0.45 (0.85)	

Baseline characteristics per quintile of white matter hyperintensities (WMH) load. The scores of the cognitive performances represent the mean z-scores (standard deviation) and median for MMSE raw scores (interquartile range)

Supplemental Table III: Automatic anatomical labeling (AAL) regions used in this study.

Abbreviations	Cortical regions	Functional division
REC	Gyrus rectus	Paralimbic
OLF	Olfactory cortex	
ORBsup	Superior frontal gyrus, orbital part	Paralimbic
ORBsupmed	Superior frontal gyrus, medial orbital	Paralimbic
ORBmid	Middle frontal gyrus orbital part	Paralimbic
ORBinf	Inferior frontal gyrus, orbital part	Paralimbic
SFGdor	Superior frontal gyrus, dorsolateral	Association
MFG	Middle frontal gyrus	Association
IFGoperc	Inferior frontal gyrus, opercular part	Association
IFGtriang	Inferior frontal gyrus, triangular part	Association
SFGmed	Superior frontal gyrus, medial	Association
SMA	Supplementary motor area	Association
PCL	Paracentral lobule	Association
PreCG	Precentral gyrus	Primary
ROL	Rolandic operculum	Association
PoCG	Postcentral gyrus	Primary
SPG	Superior parietal gyrus	Association
IPL	Inferior parietal, but supramarginal and angular gyri	Association
SMG	Supramarginal gyrus	Association
ANG	Angular gyrus	Association
PCUN	Precuneus	Association
SOG	Superior occipital gyrus	Association
MOG	Middle occipital gyrus	Association
IOG	Inferior occipital gyrus	Association
CAL	Calcarine fissure and surrounding cortex	Primary
CUN	Cuneus	Association
LING	Lingual gyrus	Association
FFG	Fusiform gyrus	Association
HES	Heschl gyrus	Primary
STG	Superior temporal gyrus	Association
MTG	Middle temporal gyrus	Association
ITG	Inferior temporal gyrus	Association
TPOsup	Temporal pole: superior temporal gyrus	Paralimbic
TPOmid	Temporal pole: middle temporal gyrus	Paralimbic
PHG	Parahippocampal gyrus	Paralimbic
ACG	Anterior cingulate and paracingulate gyri	Association
DCG	Median cingulate and paracingulate gyri	Paralimbic
PCG	Posterior cingulate gyrus	Paralimbic
INS	Insula	Paralimbic

The functional division into primary sensorimotor, paralimbic and association is based on Mesulam, 1998.

Supplemental Table IV: Graph theoretical formulae.

Measures	Formula
Strength of a node *i*	$k_i = \sum_{j \in N} a_{ij}$
Shortest path length between node *i* and *j*	d_{ij}
Global efficiency	$E_{glob}(G) = \frac{1}{N(N\text{-}1)} \sum_{i \neq j \in G} \frac{1}{d_{ij}}$
Local efficiency	$E_{loc}(G) = \frac{1}{N} \sum_{i \in G} E_{glob}(G_i)$
Clustering coefficient	$CC(G) =$
Regional nodal efficiency	$E_{reg\_nodal}(i) = \frac{1}{N\text{-}1} \sum_{i \neq j \in G} \frac{1}{d_{ij}}$
Number of shortest paths in the graph	p_{hj}
Number of shortest paths that pass through the node (*i*)	$p_{hj}(i)$
Betweenness centrality	$BC(i) = \sum_{h \neq i \neq j \in G} \frac{p_{hj}(i)}{p_{hj}}$

Supplemental Figure I. Flowchart study design.

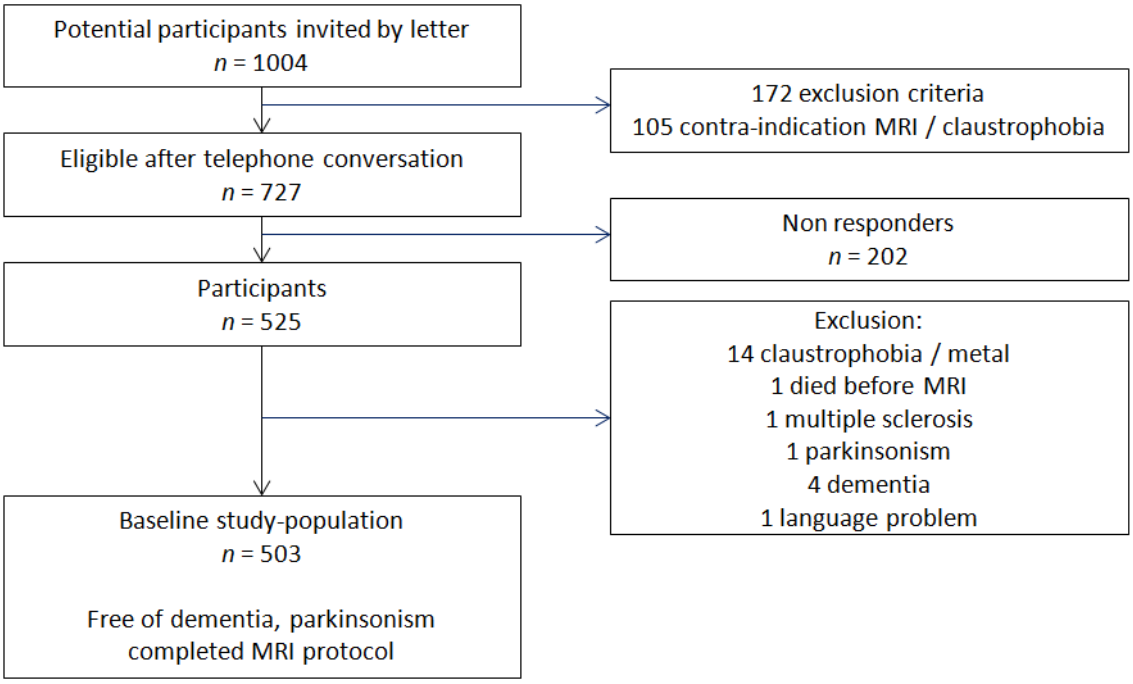

Supplemental Figure II: Cortical thickness correlation matrix.

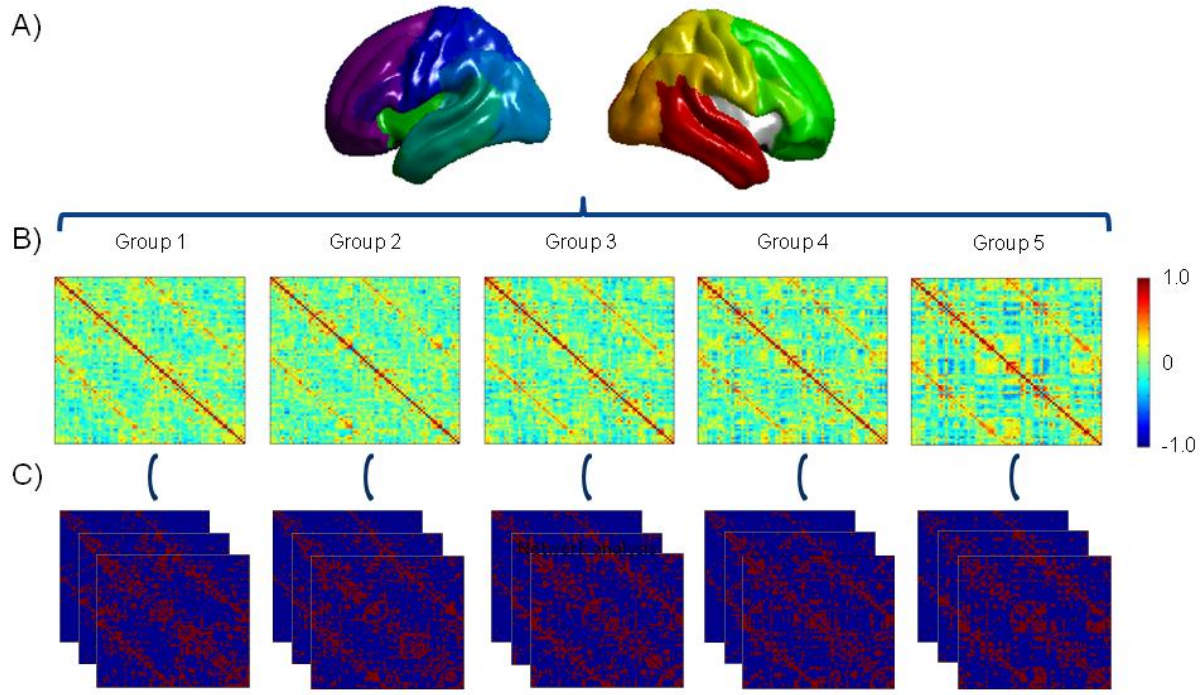

A) The cortical surface is segmented into seventy-eight automated anatomical labeling (AAL) regions (thirty-nine in each hemisphere) for each group, indicated by different colors. B) For each group, the correlation matrix is obtained after regressing out the multiple confounding factors on the cortical thickness data, such as mean cortical thickness, age and gender through multiple regression analyses. C) To investigate the graph-theoretical measures, the matrices are binarized over a wide range of density (0.05 – 0.40) to ensure that the graphs for each group have the same number of edges. In all five groups, the correlation matrices show similar structural covariance patterns on visual inspection.

Supplemental Figure III.

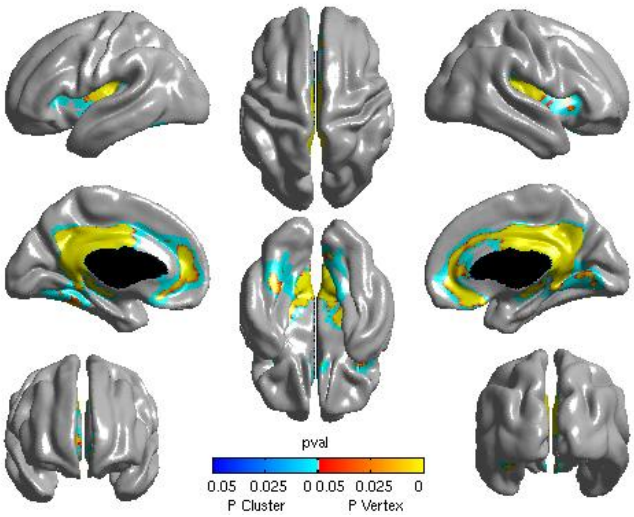

Structural covariance pattern of PCC seed ($p < 0.05$, corrected for multiple comparisons).

Supplemental Figure IV: The brain regions with the highest nodal strength, nodal efficiency and betweenness centrality for each group.

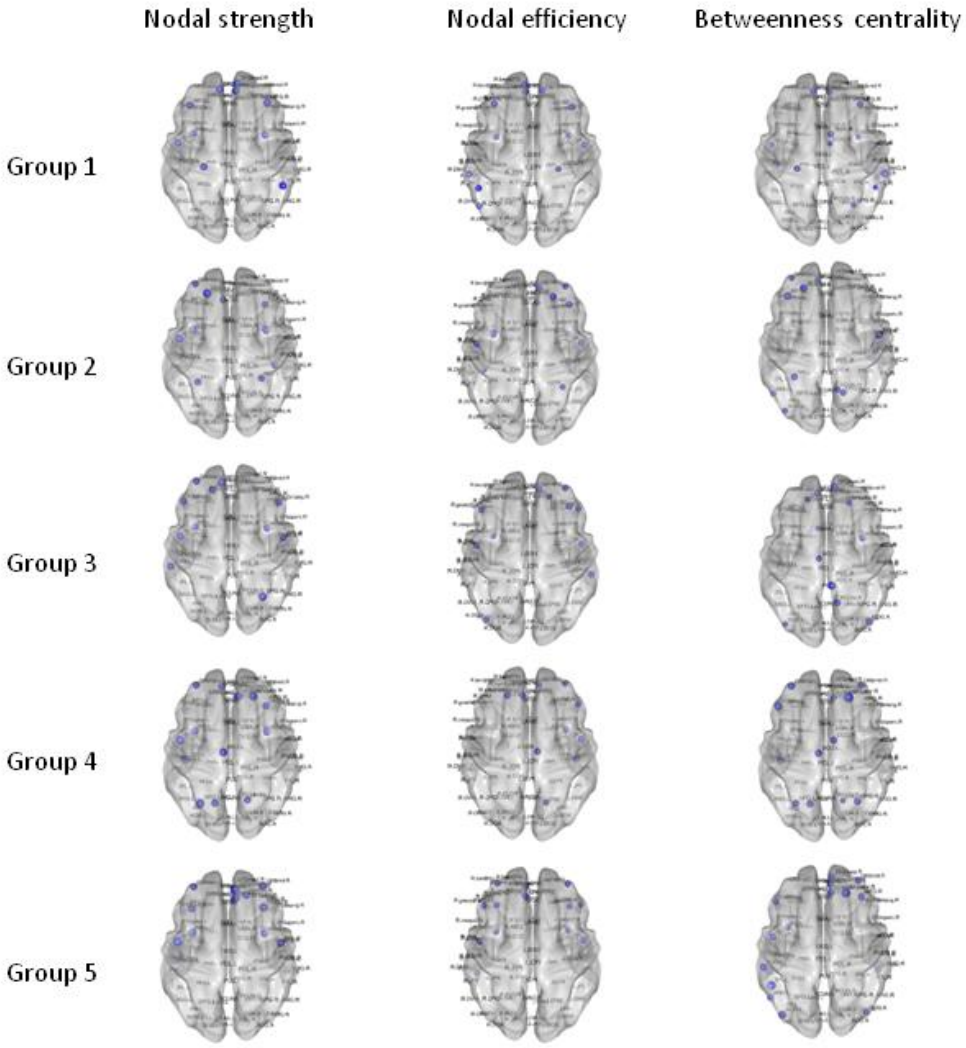

The regions are displayed if the score for the respective parameter is higher than the mean plus one standard deviation.

Supplemental Figure V. Global topological properties of the cortical thickness matrix without regressing out the overall cortical thickness out.

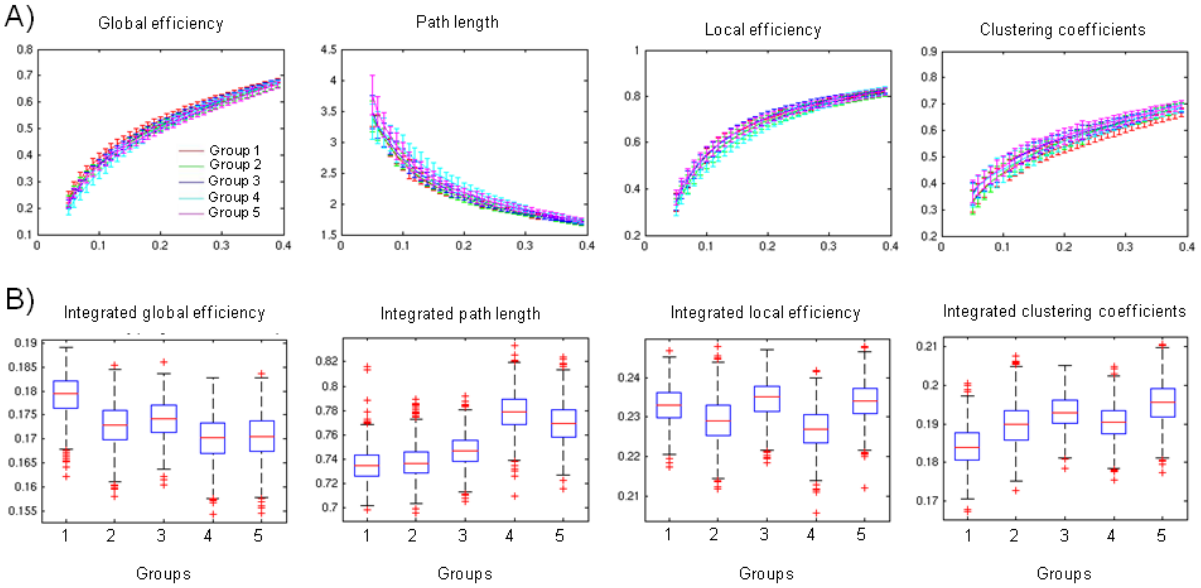

A) Global efficiency, path length, local efficiency and clustering coefficients as a function of density threshold 0.05 – 0.40 for each group. B) Integrated global efficiency, path length, local efficiency and clustering coefficients for density threshold (0.05 – 0.40) using 1000 bootstrap samples for each group. Lower integrated global efficiency with higher white matter hyperintensities load is observed, while higher integrated path length, and clustering coefficients are seen with higher white matter hyperintensities load.